NEOPLASIA
www.neoplasia.com

Volume 18 Number xx Month 2016 pp. 654–665 654

Metabolic Alterations Caused by KRAS Mutations in Colorectal Cancer Contribute to Cell Adaptation to Glutamine Depletion by Upregulation of Asparagine Synthetase[1,2]

Kosuke Toda[*], Kenji Kawada[*], Masayoshi Iwamoto[*], Susumu Inamoto[*], Takehiko Sasazuki[†], Senji Shirasawa[‡], Suguru Hasegawa[*,§] and Yoshiharu Sakai[*]

[*]Department of Surgery, Graduate School of Medicine, Kyoto University, Kyoto 606-8507, Japan; [†]Institute for Advanced Study, Kyushu University, Fukuoka, Japan; [‡]Departments of Cell Biology, Faculty of Medicine, Fukuoka University, Fukuoka, Japan; [§]Gastroenterological Surgery, Faculty of Medicine, Fukuoka University, Fukuoka, Japan

Abstract

A number of clinical trials have shown that *KRAS* mutations of colorectal cancer (CRC) can predict a lack of responses to anti-epidermal growth factor receptor–based therapy. Recently, there have been several studies to elucidate metabolism reprogramming in cancer. However, it remains to be investigated how mutated *KRAS* can coordinate the metabolic shift to sustain CRC tumor growth. In this study, we found that *KRAS* mutation in CRC caused alteration in amino acid metabolism. *KRAS* mutation causes a marked decrease in aspartate level and an increase in asparagine level in CRC. Using several human CRC cell lines and clinical specimens of primary CRC, we demonstrated that the expression of asparagine synthetase (ASNS), an enzyme that synthesizes asparagine from aspartate, was upregulated by mutated *KRAS* and that ASNS expression was induced by *KRAS*-activated signaling pathway, in particular PI3K-AKT-mTOR pathway. Importantly, we demonstrated that *KRAS*-mutant CRC cells could become adaptive to glutamine depletion through asparagine biosynthesis by ASNS and that asparagine addition could rescue the inhibited growth and viability of cells grown under the glutamine-free condition *in vitro*. Notably, a pronounced growth suppression of *KRAS*-mutant CRC was observed upon ASNS knockdown *in vivo*. Furthermore, combination of L-asparaginase plus rapamycin markedly suppressed the growth of *KRAS*-mutant CRC xenografts *in vivo*, whereas either L-asparaginase or rapamycin alone was not effective. These results indicate ASNS might be a novel therapeutic target against CRCs with mutated *KRAS*.

Neoplasia (2016) 18, 654–665

Introduction

Mutations in the *KRAS* gene are found in various types of cancer including pancreatic ductal cell adenocarcinoma (PDCA) and colorectal cancer (CRC). A number of clinical trials have shown that *KRAS* mutations in CRC can predict a lack of responses to the anti-epidermal growth factor receptor (EGFR)–based therapy. The use of anti-EGFR antibodies, cetuximab and panitumumab, is now limited to patients with *KRAS* wild-type CRC [1–3]. Therefore, the development of new therapy for CRCs with mutated *KRAS* has been desired clinically.

In recent years, there has been intense interest to understand the reprogramming of metabolism in cancer [4–7]. One of the metabolic hallmarks of malignant tumor cells is their dependency on aerobic glycolysis, known as the Warburg effect [4,5]. The role of KRAS signaling in the regulation of aerobic glycolysis has been reported in several types of cancer, although the molecular mechanism behind the

Abbreviations: CRC, colorectal cancer; ASNS, asparagine synthetase.

Address all correspondence to: Kenji Kawada, MD, PhD, Department of Surgery, Graduate School of Medicine, Kyoto University, 54 Shogoin- Kawara-cho, Sakyo-ku, Kyoto, Japan, 606-8507.
E-mail: kkawada@kuhp.kyoto-u.ac.jp

[1] Grant supports: This work was supported by grants from the Ministry of Education, Culture, Sports, Science, and Technology of Japan and from the Laboratory for Malignant Control Research, Medical Innovation Center, Kyoto University Graduate School of Medicine (to K. Kawada).
[2] Potential conflict of interest: No potential conflicts of interest were disclosed.
Received 15 July 2016; Revised 23 September 2016; Accepted 26 September 2016

© 2016 The Authors. Published by Elsevier Inc. on behalf of Neoplasia Press, Inc. This is an open access article under the CCBY-NC-ND license (http://creativecommons.org/licenses/by-nc-nd/4.0/). 1476-5586
http://dx.doi.org/10.1016/j.neo.2016.09.004

upregulation of glucose metabolism is yet to be elucidated. For example, in a PDCA mouse model, mutated *KRAS* was shown to maintain tumor growth by stimulating glucose uptake and channeling glucose intermediates into the hexosamine biosynthesis pathway (HBP) and pentose phosphate pathway (PPP) [8]. Notably, knockdown of rate-limiting enzymes in HBP or PPP suppressed tumor growth, indicating their potential as therapeutic targets. In CRC cells, the increase of glucose transporter 1 (GLUT1) expression and glucose uptake was critically dependent on *KRAS* or *BRAF* mutations [9]. Fluorodeoxyglucose (FDG) positron emission tomography scans are used to evaluate glucose metabolism by measuring the uptake of FDG, a glucose analog. We previously reported that CRC cells with mutated *KRAS* increased FDG accumulation by upregulation of GLUT1 [10–12]. However, it remains to be investigated how mutated *KRAS* can coordinate the metabolic shift to sustain tumor growth and whether specific metabolic pathways are essential for the *KRAS* mutation-mediated tumor maintenance in CRC.

In addition to their glucose dependency, malignant cells rely on glutamine to support cell growth and survival [13,14]. Glutamine is one of the most heavily consumed nutrients by cells in culture and the most abundant amino acid in circulation [15]. Once imported into the cells, glutamine serves as a carbon source for the tricarboxylic acid (TCA) cycle and a nitrogen source for nucleotide and nonessential amino acids. In purine and pyrimidine biosynthesis, glutamine donates its amino group and is subsequently converted to glutamate. In turn, glutamate serves as the primary nitrogen source for other nonessential amino acids by providing the amino group and is subsequently converted to α-ketoglutarate. The glutamine-derived α-ketoglutarate replenishes the TCA cycle by providing oxaloacetate that condenses with acetyl-CoA to maintain the TCA cycle and support *de novo* fatty acid biosynthesis. In addition to providing carbons and nitrogens for biosynthesis, glutamine is also involved in other cellular processes, including antioxidative stress and the mammalian target of rapamycin (mTOR) signaling. The spectrum of glutamine-dependent tumors and the mechanisms by which glutamine supports cancer metabolism are being actively investigated [13–18]. In the PDCA mouse model, glutamine supports the growth of pancreatic cancer through an oncogenic *KRAS*-regulated metabolic pathway [19]. Most cells utilize glutamine dehydrogenase (GLUD1) to convert glutamine-derived glutamate into α-ketoglutarate in the mitochondria to fuel the TCA cycle. However, PDCA cells rely on a distinct pathway in which glutamine-derived aspartate is transported into the cytoplasm and converted to oxaloacetate by aspartate transaminase (GOT1). In glioma and neuroblastoma, asparagine plays a critical role in regulating cellular adaptation to glutamine depletion [20]. Asparagine was shown to be necessary and sufficient to suppress apoptosis induced by the glutamine withdrawal without restoring the levels of other nonessential amino acids or TCA cycle intermediates. Asparagine synthetase (ASNS), the enzyme that synthesizes *de novo* asparagine from aspartate and glutamine, was required to suppress glutamine withdrawal–induced apoptosis, and its expression was statistically correlated with poor prognosis.

The present study aimed to investigate how mutated *KRAS* could regulate metabolic reprograming in CRC and whether metabolic enzymes associated with mutated *KRAS* could be novel therapeutic targets for CRC with *KRAS* mutations. Given that cancer cells rely on changes in metabolism to support their growth and survival, targeting the metabolism is a potential cancer treatment strategy. There are a few reports regarding *KRAS* mutation-related metabolic alterations in CRC. Here, we revealed that mutated *KRAS* upregulated ASNS expression through the PI3K-AKT-mTOR pathway and that ASNS maintained cell adaptation to glutamine depletion through asparagine biosynthesis in *KRAS*-mutant CRCs. Notably, tumor growth of *KRAS*-mutant CRC cells was significantly suppressed upon ASNS knockdown. These results indicate that ASNS might be a novel therapeutic target for CRCs with mutated *KRAS*. To our knowledge, this is the first study to investigate amino acid metabolism associated with *KRAS* mutation in CRC.

Materials and Methods

Cell Lines and Reagents

All lines were maintained in Dulbecco's modified Eagle medium (DMEM) (glucose 25 mM, glutamine 4 mM) (043-30085, Wako) containing 10% FBS. Media without glutamine were prepared by using glutamine-free DMEM (glucose 25 mM, glutamine 0 mM) (043-32245, Wako) containing 10% FBS. LoVo, RKO, COLO-205, and WiDR cells were supplied from American Type Culture Collection. The identity of cell line was confirmed by short tandem repeat analysis (Takara Bio). HCT116, HKh-2, HKe-3, DLD-1, and DKO-4 cell lines were generated as described previously [21]. All amino acid were obtained from Wako. U0126 was purchased from Calbiochem; LY294002 and rapamycin were from Wako.

Measurement of Metabolites

In cell samples, 1×10^6 cells were seeded in 10-cm dishes in DMEM (25 mM glucose, 4 mM glutamine) containing 10% FBS for 48 hours. Metabolome analysis was conducted by C-SCOPE package of Human Metabolome Technologies, Inc., using capillary electrophoresis (CE) time-of-flight mass spectrometry for cation analysis and CE tandem mass spectrometry for anion analysis as described previously [11].

Quantitative Reverse Transcription Polymerase Chain Reaction (RT-PCR) Analysis

Total RNAs were extracted and reverse transcription was performed with oligo (dT) primer and Transcriptor First Strand cDNA Synthesis Kit (Roche) according to the manufacturer's instructions. The resulting cDNA was quantified using StepOnePlus Real-Time PCR System (Applied Biosystems) and THUNDERBIRD SYBR qPCR Mix (TOYOBO). Primer sequences are found in Supplementary Table 1. All transcription levels were normalized to that for *ACTB*.

Western Blot Analysis

Cells and tissue samples were lysed in lysis buffer (50 mM Tris-HCl, 150 mM NaCl, 1 mM EDTA, 50 mM NaF, 1% NP40) supplemented with inhibitor cocktails of protease and phosphatase. Primary antibodies were mouse monoclonal anti-KRAS (Santa Cruz Biotechnology), rabbit polyclonal anti-ASNS (Abcam), rabbit monoclonal anti–pohospho-p44/42 kinase (Thr202/Tyr204) (Cell Signaling), rabbit monoclonal anti-p44/42 kinase (Cell Signaling), rabbit monoclonal anti–phospho-Akt (Ser473) (Cell Signaling), rabbit monoclonal anti-Akt (Cell Signaling), rabbit polyclonal anti–phospho-p70 S6 kinase (Thr389) (Cell Signaling), rabbit polyclonal anti-p70 S6 kinase (Cell Signaling), and mouse monoclonal anti–β-actin-peroxidase (Sigma-Aldrich).

RNA Interference

To knock down the endogenous expressions of both *KRAS* and *CS*, FlexiTube GeneSolutions (Qiagen) for *KRAS* (#1: SI03101903, #2: SI03106824) and *CS* (#1: SI04147997, #2: SI04184796) were employed,

and AllStars negative control (NC) small interfering RNA (siRNA) was used for nonsilencing control. The siRNA (10 nM) was transfected with Lipofectamine RNAiMAX (Invitrogen) according to the manufacturer's instruction.

Cell Proliferation Assay

A cell proliferation assay was performed with Cell Counting Kit-8 (CCK-8, Dojindo) according to the manufacturer's instruction. Cells were cultured in 96-well plates at a density of 5000 cells/well for 48 to 72 hours with or without treatment.

Clonogenic Assay

Cells were seeded in 6-well plates at a density of 200 cells/well in DMEM (25 mM glucose, 4 mM glutamine) containing 10% FBS. Ten days later, colonies were fixed in 1% glutaraldehyde and stained with 0.2% crystal violet for 30 minutes. A colony was defined as a cluster of at least 50 cells.

Construction of Recombinant Lentivirus

The following oligonucleotides were used to knock down *ASNS* expression: sh*ASNS*#1-sense, 5′-CCGGATGGTGAAATCTACAACCATACTCGAGTATGGTTGTAGATTTCACCATTTTTTG-3′;sh*ASNS*#1-antisense, 5′-AATTCAAAAAATGGTGAAATCTACAACCATACTCGAGTATGGTTGTAGATTTCACCAT-3′;sh*ASNS*#2-sense, 5′-CCGGTTAGGTGGTCTTTATGCTGTACTCGAGTACAGCATAAAGACCACCTAATTTTTG-3′;sh*ASNS*#2-antisense, 5′-AATTCAAAAATTAGGTGGTCTTTATGCTGTACTCGAGTACAGCATAAAGACCACCTAA-3′. Each set of oligonucleotides was annealed and cloned into the AgeI/EcoRI sites of pLKO.1 (Addgene). pLKO.1-TRC control vector (Addgene) was used as control. *ASNS* cDNA was obtained from HCT116 cells. The *ASNS* cDNA was cloned into the pLVSIN-CMV (TaKaRa BIO).

Apoptosis Assay

In terminal deoxynucleotidyl transferase-mediated dUTP-FIFC nick end-labeling (TUNEL) assay, cells were cultured under glutamine-free DMEM (25 mM glucose, 0 mM glutamine) containing 10% FBS for 72 hours and then fixed in 4% parafolmaldehyde. The number of TUNEL-positive cells in each of the three slides was counted in five random fields (magnification, ×400) by software BZ-H3C (Keyence) and expressed as a percentage of the total cells counted. The activity of caspase-3 and -7 was measured by using caspase-Glo 3/7 assay (Promega) according to the manufacturer's protocol. Caspase activity was normalized to the cell number counted by CCK-8 cell proliferation assay under the same density and conditions.

Animal Tumor Model

We subcutaneously injected 4-6 × 10^6 cancer cells into flanks of 4- to 6-week-old female KSN/slc nude mice (JAPAN SLC). Tumor volumes were calculated using the formula $(L \times W^2) \times 0.5$, where L is length and W is width. At the time of L-asparaginase (L-Asp) and rapamycin treatment, tumors were established in KSN/slc nude mice by subcutaneous injection of 5 × 10^6 of HCT116. Mice with tumors of 150 to 300 mm^3 were randomly divides into 4 groups. L-Asp (Kyowa Hakko Kirin Co., Ltd.) was injected daily intraperitoneally at 1500 U/kg for 15 days [22]. Rapamycin (LC Laboratories) was dosed in 4% ethanol/5% PEG400/5% Tween 80 in water for injection solution and injected every 5 days intraperitoneally at 3 mg/kg [23]. The control group was injected every 5 days with an equal volume of the vehicle. Mice were ethically sacrificed when mean tumor volume reached 2000 mm^3. Animal experimental studies were conducted in accordance with our institutional guidelines and approved by the Kyoto University Animal Care Committee.

Immunohistochemistry

Formalin-fixed, paraffin-embedded sections were stained with anti-rabbit ASNS (Abcam), anti-mouse CD34 (Abcam), or ant-mouse Ki67 (Dako) antibody. Antigen retrieval was achieved with microwave in citrate buffer (pH: 6.0). The Ki67-positive cell numbers were counted in five random fields (×400). For primary CRC tissue, ASNS immunoreactivity score was determined by the sum of distribution and staining intensity, as previously described [24]. ASNS expression was defined as low (total score 0-3) or high (total score 4-7). The distribution was scored based on the positivity rate as "0" (0%-5%), "1" (5%-25%), "2" (25%-50%), "3" (50%-75%), or "4" (>75%). The staining intensity was scored as "0" (no staining), "1" (weakly stained), "2" (moderately stained), or "3" (strongly stained). Two researchers (K.T. and S.I.) independently evaluated all immunohistochemistry samples without prior knowledge of other data. The slides with different evaluations among them were reinterpreted at a conference to reach the consensus.

Patients, Clinicopathological Data

A total of 93 CRC samples were collected from patients who underwent tumor resection and with *KRAS* status checked at Kyoto University Hospital between April 2009 and September 2013. No patients received preoperative chemotherapy and radiation therapy. This study protocol was approved by the institutional review board of Kyoto University, and patients provided their written consent for data handling.

Statistical Analysis

The statistical significance of differences was determined by Student's t test or χ^2 test. All values were expressed as mean ± standard deviation (SD). All analyses were two-sided, and differences with a P value of less than .05 were considered statistically significant in all analyses. Statistical analyses were conducted with the JMP software (version 9, SAS Institute, Inc.).

Results

KRAS Mutation-Related Alterations of Amino Acid Metabolism in Human CRC Cells

To investigate the specific pathway by which mutated *KRAS* exhibits metabolic alterations, we used human CRC cell lines with mutated *KRAS* (HCT116 and DLD-1) and their isogenic lines in which the endogenous mutant *KRAS* allele was disrupted through targeted homologous recombination [11,21]. HKh-2 and HKe-3 are two independent HCT116 clones with the mutated *KRAS* disrupted; similarly, DKO-4 is a DLD-1 clone with the mutated *KRAS* disrupted. These paired cell lines essentially differ only in the mutational status of *KRAS* gene, which allowed us to investigate the function of normal or mutant KRAS proteins at physiological, normally regulated levels. In addition, these CRC lines also harbor additional mutations in *CTNNB1* and *TGFβ-RII* genes [25,26]; therefore, *KRAS* signaling can be studied in the context of other gene mutations commonly found in CRC. Using these paired lines, we previously reported that mutated *KRAS* caused higher FDG accumulation by upregulation of glucose uptake through GLUT1 [10–12]. To further dissect the metabolic alterations caused by mutated *KRAS*, CE mass spectrometry (CE/MS) metabolomic analysis was performed to comprehensively characterize intracellular metabolites in HCT116 paired lines. This analysis revealed

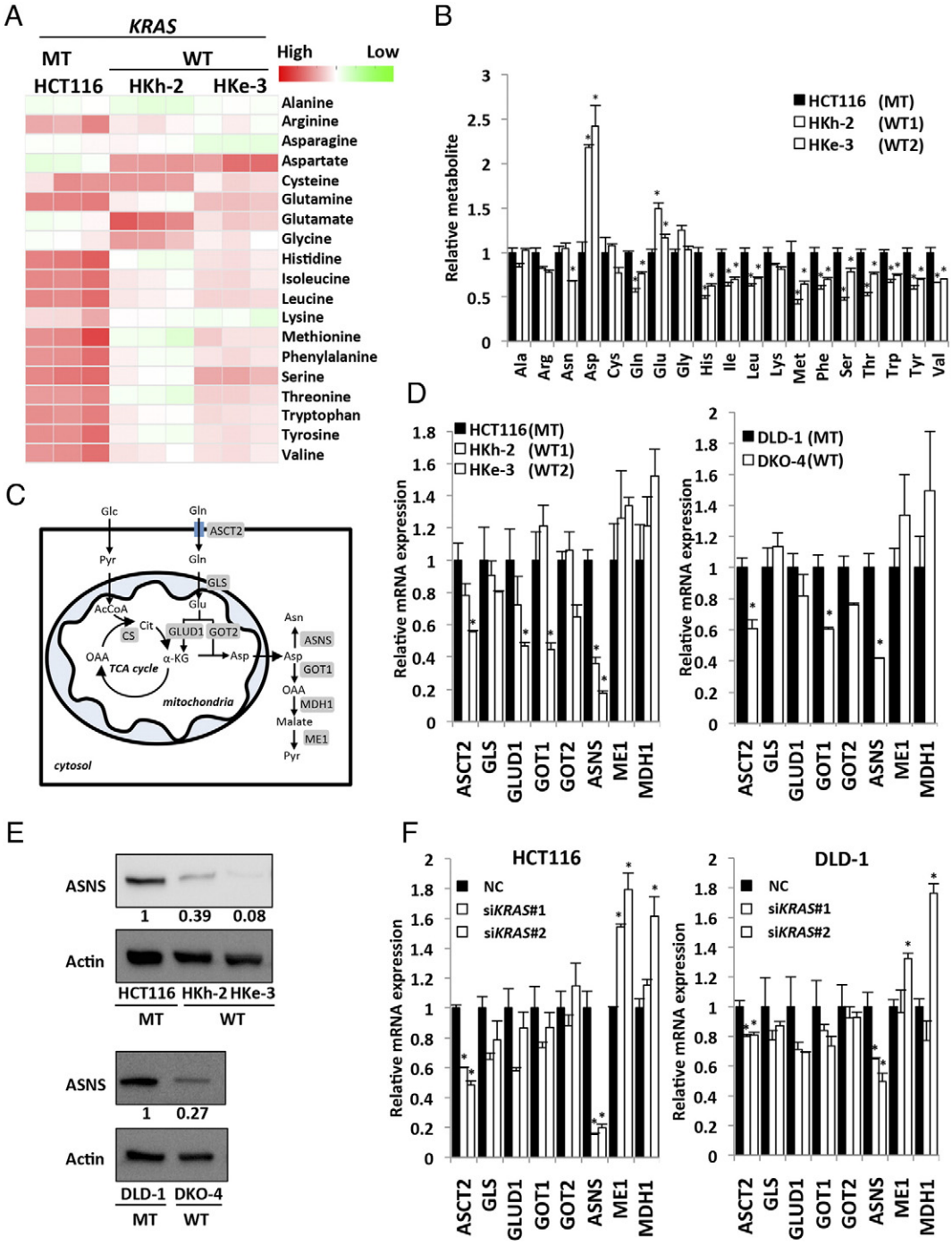

Figure 1. Metabolic alterations caused by *KRAS* mutations in colorectal cancer cells. (A) Heat map shows metabolic changes of amino acid in *KRAS*-mutant CRC cells (HCT116) and their isogenic counterparts containing wild-type *KRAS* allele (HKh-2 and HKe-3). Metabolome analysis (CE/MS) was performed from triplicates for each condition and normalized to cell number. Cells were maintained in DMEM (25 mM glucose, 4 mM glutamine) containing 10% FBS for 48 hours. WT, *KRAS* wild type; MT, *KRAS* mutant. (B) Relative metabolite levels are expressed as fold change compared with metabolite concentration of HCT116. Mean; *bars,* ± SD, $n = 3$ (Student's *t* test; $^*P < .05$). Ala, alanine; Arg, arginine; Asn, asparagine; Asp, aspartate; Cys, cysteine; Gln, glutamine; Glu, glutamate; Gly, glycine; His, histidine; Ile, isoleucine; Leu, leucine; Lys, lysine; Met, methionine; Phe, phenylalanine; Ser, serine; Thr, Threonine; Trp, tryptophan; Tyr, tyrosine; Val, valine. (C) Schematic representation of glutamine metabolism. α-KG, α-ketoglutarate; OAA, oxaloacetate; Pyr, pyruvate; Glc, glucose; AcCoA, acetyl-CoA; Cit, citrate. (D) Quantitative RT-PCR showing relative mRNA levels for metabolic enzymes associated with glutamine metabolism. *KRAS*-mutant cells (HCT116 and DLD-1) and their isogenic counterpart containing wild-type *KRAS* allele (HKh-2, HKe-3, and DKO-4). Mean; *bars,* ± SD, $n = 3$ (Student's *t* test; $^*P < .05$). (E) Western blot photographs of ASNS and β-actin (Actin) (*top*) and quantified data for ASNS (*bottom*) (normalized with β-actin). (F) Quantitative RT-PCR showing relative mRNA levels for metabolic enzymes associated with glutamine metabolism. HCT116 cells (left) and DLD-1 cells (right) were treated separately with two independent siRNA constructs (#1 and #2) targeting *KRAS* and NC siRNA. Mean; *bars,* ± SD, $n = 3$ (Student's *t* test; $^*P < .05$).

that mutated *KRAS* induced changes in multiple metabolic pathways such as glycolysis, PPP, TCA, and most significantly the amino acid pathway (Figure 1*A* and Supplementary Figure S1*A*). In particular, aspartate level in HCT116 with mutated *KRAS* was significantly lower compared with that in their isogenic counterparts containing wild-type *KRAS* allele (HKh-2 and HKe-3). In contrast, asparagine level was significantly higher in HCT116 than in HKe-3 (Figure 1*B*). The asparagine/aspartate ratio was significantly higher in HCT116 than in HKh-2 and HKe-3 (Supplementary Figure S1*B*).

Upregulation of Asparagine Synthetase in KRAS-Mutant CRCs Through the PI3K-AKT-mTOR Pathway

Recently, it has been reported that *KRAS* mutation in PDCA cells regulates the glutamine metabolism through its conversion to aspartate, thereby supporting tumor growth by maintaining the cellular redox balance [19]. Glutamine is transported into the cytoplasm by neutral amino acid transporter (ASCT2) and is subsequently converted to glutamate by glutaminase (GLS) at mitochondria. Thereafter, glutamate can be converted to α-ketoglutarate by GLUD1 to replenish the TCA cycle by GLUD1 or converted to nonessential amino acids such as aspartate and alanine by transaminases. In PDCA, glutamic-oxaloacetic transaminase 2 (GOT2) was identified as the transaminase associated with mutated *KRAS* at mitochondria [19]. Glutamine-derived aspartate is transported into the cytoplasm where it can be converted to asparagine by ASNS or to pyruvate by GOT1, malic enzyme 1, and malate dehydrogenase 1 (Figure 1*C*). A recent report demonstrated that mutated *KRAS* controlled the reprograming of glutamine metabolism by decreasing GLUD1 and increasing GOT1 in PDCA [19]. To identify the metabolic enzymes associated with the reprograming of glutamine metabolism in CRC, we first screened the expression of the above-mentioned enzymes by quantitative RT-PCR analysis. Notably, *ASNS* mRNA expression in the parental *KRAS*-mutant cells (HCT116 and DLD-1) was about 2.5- to 5-fold higher than in their isogenic wild-type *KRAS* cells (Figure 1*D*). By Western blotting, we also confirmed that ASNS protein level was about 2.5- to 10-fold higher in the parental *KRAS*-mutant cells than in the corresponding isogenic wild-type *KRAS* cells (Figure 1*E*). To further validate the relationship between ASNS and KRAS, we performed RNA interference experiments. We introduced two kinds of different siRNA constructs targeting *KRAS* (referred to as si*KRAS*#1 and #2) into HCT116 and DLD1 cells (Supplementary Figure S2*A* and *B*) and verified that both si*KRAS* constructs dramatically decreased mRNA expression of *ASNS* but not *GLUD1* or *GOT1* (Figure 1*F*).

KRAS protein activates its downstream signaling pathways, such as the Raf/MEK/ERK and PI3K/Akt pathways, leading to malignant transformation. We used a specific inhibitor of each pathway to examine which pathway regulates the induction of ASNS expression mediated by mutated *KRAS*. HCT116 and DLD-1 cells were treated with a MEK inhibitor (U0126, 20 μM), a PI3K inhibitor (LY294002, 50 μM), or an mTOR inhibitor (rapamycin, 20 nM). A Western blot analysis showed that ASNS expression was dramatically inhibited by LY294002 and rapamycin but not U0126 (Figure 2*A*), suggesting that ASNS expression is correlated with the PI3K/AKT/mTOR pathway in *KRAS*-mutant cells (HCT116 and DLD-1).

Based on these findings, we hypothesized that ASNS expression in CRC is regulated by mutated *KRAS*. We therefore determined the expression level of ASNS in several human CRC cell lines. HCT116, DLD-1, and LoVo cells bear a mutant *KRAS* allele at codon 13 (G13D), whereas RKO, COLO-205, and WiDr cells bear the wild-type *KRAS*. A Western blot analysis showed that *KRAS*-mutant cells constitutively expressed high level of ASNS, whereas wild-type *KRAS* cells exhibited little to no ASNS expression (Figure 2*B*). To further investigate the relationship between *KRAS* status and ASNS expression, we next examined clinical specimens of human primary CRC by immunohistochemistry. Representative cases of CRCs bearing mutated and wild-type *KRAS* are shown in Figure 2*C*. Of a total of 93 primary CRC patients, 50% (46 of 93) were high for ASNS, whereas 50% (47 of 93) were low (Table 1). Patients were classified into two groups based on their *KRAS* mutational status: patients with mutated *KRAS* (n = 39) and those with wild-type *KRAS* (n = 54). ASNS expression was high in 74% (29 of 39) of patients with mutated *KRAS*, whereas it was low in 31% (17 of 54) of those with wild-type *KRAS*, with a significant correlation between mutated *KRAS* and ASNS expression (odds ratio, 6.31; $P < .001$, Figure 2*D*). ASNS expression was not correlated with age, sex, tumor location, tumor size, T-category, N-category, and M-category (Table 1). Taken together, *KRAS* status is one of the key regulators of ASNS expression in CRC.

The Role of ASNS in Cell Adaptation to Glutamine Depletion in KRAS-Mutant CRC Cells

ASNS is the enzyme that synthesizes *de novo* asparagine from aspartate using glutamine as a nitrogen source. In human glioma and neuroblastoma, it was recently reported that asparagine was essential to suppress apoptosis induced by glutamine withdrawal without restoring the levels of other nonessential amino acids or TCA cycle intermediates and that ASNS knockdown led to cell death even in the presence of glutamine [20]. To evaluate whether *KRAS* mutational status of CRC cells could affect their addiction to glutamine, we tested the clonogenic assay. In the absence of glutamine, colony number of *KRAS*-mutant cells (HCT116) was significantly higher than the isogenic wild-type *KRAS* cells (HKh-2 and HKe-3) (Figure 3*A*), indicating that *KRAS*-mutant CRC cells were more resistant to glutamine deprivation than wild-type *KRAS* CRC cells. Citrate synthase (CS) is a TCA cycle enzyme that catalyzes the formation of citrate from oxaloacetate and acetyl-CoA. CS siRNA was identified to be a suppressor of glutamine withdrawal–induced apoptosis by reducing TCA cycle activity and redirecting oxaloacetate for synthesis of aspartate and asparagine [20]. Consistent with the findings in human glioma and neuroblastoma, we found that CS knockdown using siRNA prevented glutamine withdrawal–induced apoptosis and suppression of cell proliferation in HCT116 cells (Supplementary Figure S3, *A*–*C*), although CS expression level was not correlated with *KRAS* mutation (Supplementary Figure S3*D*). These data further support the critical role of this pathway in glutamine metabolism and tumor growth.

To further investigate the role of ASNS, two lentiviral shRNA constructs targeting *ASNS* (referred to as sh*ASNS*#1 and sh*ASNS*#2) were introduced into HCT116 cells (Supplementary Figure S4*A*). Under the condition of glutamine depletion, both sh*ASNS* constructs significantly decreased cell proliferation compared with the control in a dose-dependent manner (Figure 3*B*), although cell proliferation was not affected under sufficient amount of glutamine (4 mM Gln) (Supplementary Figure S4*B*). Similarly, under the glutamine-free condition, the colony number of sh*ASNS* transfectants was significantly lower than that of the control cells in the clonogenic assay (Figure 3*C*). We also found that the number of apoptotic cells was significantly higher in sh*ASNS* transfectants than the control cells (Supplementary Figure S4*C*). To test whether these effects of shRNAs were specific, we further performed rescue experiments. Namely, the

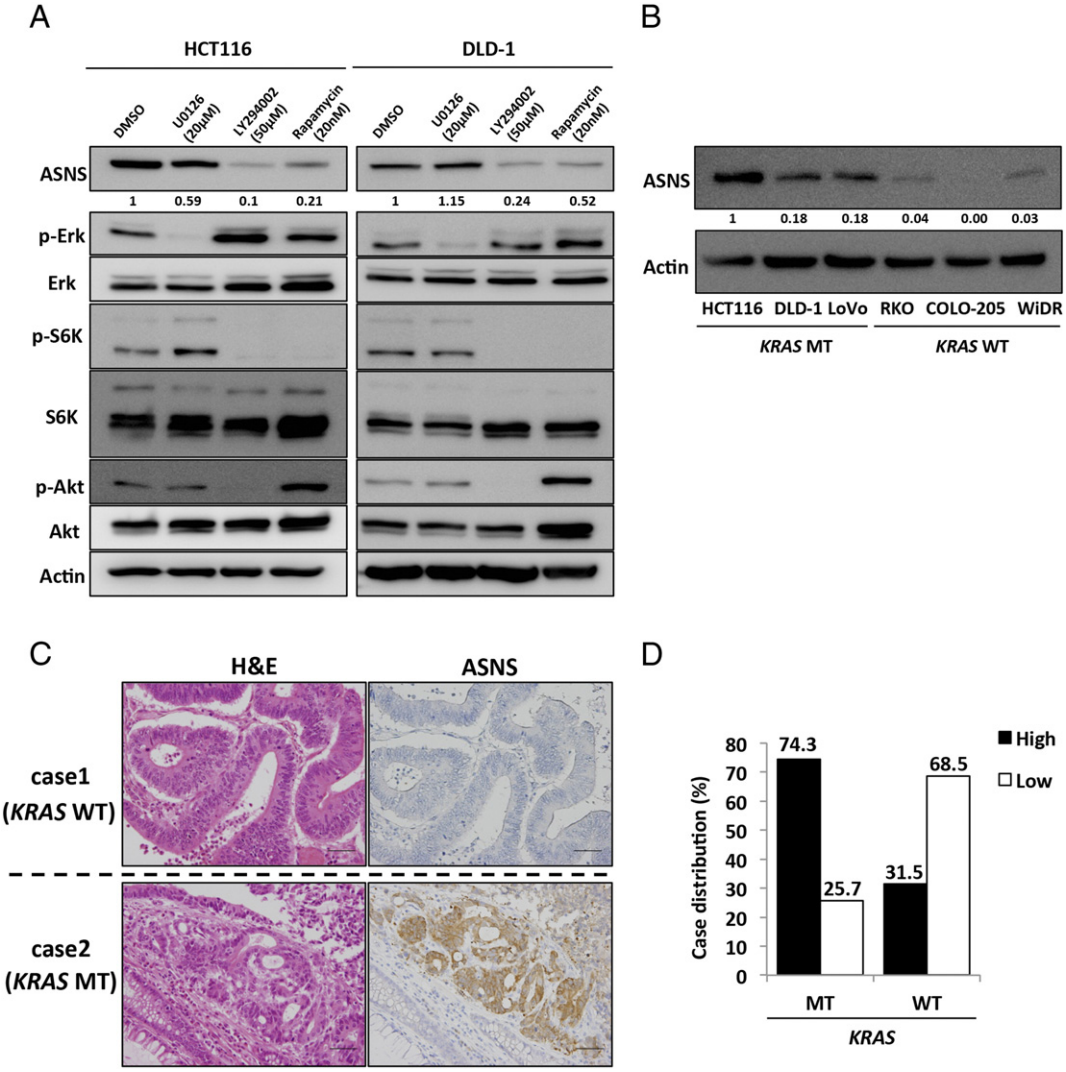

Figure 2. ASNS expression in CRC. (A) Western blot analyses of HCT116 (left) and DLD-1 (right) treated with dimethyl sulfoxide (DMSO), 20 μM U0126 (MEK inhibitor), 50 μM LY294002 (PI3K inhibitor), or 20 nM rapamycin (mTOR inhibitor) for 48 hours. Protein levels were normalized to β-actin (Actin). Densitometry values were expressed as fold change compared with DMSO treating cells. (B) Western blot analysis of ASNS expression in several human CRC cell lines. Densitometry values were expressed as fold change compared with HCT116. (C) H&E and immunohistochemical staining for ASNS in primary CRCs. Upper panels show serial sections of a *KRAS*-mutant CRC case, whereas lower panels show those of a wild-type *KRAS* one. Scale bar, 50 μm. (D) Relationship between *KRAS* mutational status and ASNS expression in 93 primary CRC samples.

ASNS expression plasmid (pLVSIN-*ASNS*) was transfected into sh*ASNS*#2 cells in which the targeted sequence was located at the 3′-untranslated region (3′UTR) (Supplementary Figure S4*D*). Both the proliferation rate and clonogenic growth of sh*ASNS* transfectants under the glutamine-free condition were significantly rescued by ASNS overexpression (Supplementary Figure S4, *E* and *F*). To evaluate whether the growth-inhibitory effects of sh*ASNS* constructs were recovered by exogenous addition of asparagine (the ASNS product), we next tested the effect of asparagine addiction to the medium and found that 0.1 mM asparagine was sufficient to recover the growth inhibition of sh*ASNS* transfectants in the cell proliferation (Figure 3, *D* and *E*) and clonogenic assays (Supplementary Figure S5*A*). Consistently, asparagine addition significantly suppressed the apoptosis of sh*ASNS* transfectants under the glutamine-free condition (Figure 3*F*). Furthermore, we found that the significant growth recovery of sh*ASNS* transfectants under the glutamine-free condition was observed only upon asparagine addition but not other amino acids (Figure 3*G*), indicating the specificity of asparagine-mediated rescue of cell survival. Together, these data indicate that ASNS upregulation caused by *KRAS* mutation maintains cell adaptation to glutamine depletion through asparagine biosynthesis.

Suppression of Tumor Growth In Vivo of KRAS-Mutant CRC Cells by ASNS Inhibition

As further investigation of the importance of ASNS in *KRAS*-mutant CRC cells, we assessed the ability of CRC cells to grow as xenografts *in vivo*. Consistent with results obtained from the *in vitro* studies, sh*ASNS*#1 construct significantly reduced tumor growth of HCT116 cells compared with the control cells (Figure 4*A* and Supplementary Figure S4*G*). Immunohistochemical analysis indicated that the number of Ki67-positive tumor cells was significantly lower in sh*ASNS*#1 transfectant tumors than in the control tumors, especially in the location

Table 1. Univariate Analysis of Factors Associated With Expressions of ASNS

	ASNS		
	High (n = 46)	Low (n = 47)	*P*
Mean, age ± SD (y)	69.5 ± 10.7	69.5 ± 10.8	.63
Sex			
Male	28	27	.84
Female	18	20	
Location			
Colon	32	33	1
Rectum	14	14	
Mean tumor size (mm)			.26
≥50	24	19	
<50	22	28	
UICC-TMN stage			
I/II	20	27	.22
III/IV	26	20	
T-category			
Negative	12	12	1
Positive	34	35	
M-category			
Negative	39	39	1
Positive	7	8	
N-category			
Negative	22	29	.21
Positive	24	18	
KRAS			
Wild type	17	37	<.001
Mutated	29	10	

distant from the CD34-positive tumor blood vessels (Figure 4, *B* and *C*). We also measured the intratumoral vessel density and found no difference between sh*ASNS*#1 transfectant tumors and the control (Figure 4*D*). Furthermore, we also performed rescue experiments *in vivo* and found that the reduced tumor growth of sh*ASNS*#2 transfectant was significantly recovered by ASNS overexpression (Supplementary Figure S5*B)*.

Combination Treatment of L-Asp Plus Rapamycin

Given the importance of glutamine metabolism in the maintenance of tumor growth, we speculated that *KRAS*-mutant CRC cells might be sensitive to the inhibition of anabolic glutamine metabolism. Therefore, we determined whether ASNS inhibition combined with depletion of plasma glutamine and asparagine could be used as a novel therapeutic strategy to treat *KRAS*-mutant CRCs. L-Asp, an FDA-approved drug widely used to treat acute lymphoblastic leukemia (ALL), has activities of both asparaginase and GLS [27,28]. The inhibitory effect of L-Asp on the cell proliferation and clonogenic growth *in vitro* was significantly higher in sh*ASNS* transfectants than in the control cells (Figure 5, *A* and *B*). A potent ASNS inhibitor capable of inhibiting the intracellular asparagine biosynthesis *in vivo* is yet to be developed [20,29,30]. We found that the upregulation of ASNS expression mediated by the mutated *KRAS* was dramatically suppressed by rapamycin (Figure 2*A*), and so we examined whether rapamycin could synergize with L-Asp in the clonogenic assay. In both the clonogenic and cell proliferation assays, the combination of L-Asp plus rapamycin suppressed cell growth of *KRAS*-mutant CRCs (HCT116 and DLD-1) more prominently than L-Asp or rapamycin alone did (Figure 5, *C* and *D*). We next assessed the sensitivity of HCT116 xenografts to the combination of L-Asp plus rapamycin *in vivo*. Mice with tumors of 150 to 300 mm^3 were randomly divided into 4 groups and treated with vehicle, L-Asp alone (1500 U/kg), rapamycin alone (3 mg/kg), or the combination of both drugs. Consistent with the *in vitro* results, tumor growth of xenografts was strongly suppressed by the combination of L-Asp plus rapamycin, although treatments using each single drug showed no or marginal effect (Figure 5*E*). We examined ASNS expression *in vivo* of each xenograft and confirmed that rapamycin significantly suppressed ASNS expression, whereas L-Asp upregulated its expression (Supplementary Figure S6, *A* and *B*). Taken together, these results indicate that the combination therapy using L-Asp plus ASNS inhibitor could be an effective strategy to treat *KRAS*-mutant CRC by impairing the glutamine metabolism.

Discussion

Metabolic alterations have recently emerged as one of the cancer hallmarks [4–7]. Major tumor suppressors and oncogenes have intimate connections with the metabolic pathways. *KRAS* mutations occur in a variety of human malignancies, most frequently in PDCA, non–small cell lung cancer, and CRC. Recent studies indicate that the role of *KRAS* in cancer metabolism is complex [31,32]. In an inducible $KRAS^{G12D}$-driven PDCA mouse model, $KRAS^{G12D}$ played a vital role in controlling tumor metabolism by increasing glucose uptake, which resulted in activation of protein glycosylation and ribose biogenesis through the HBP and nonoxidative PPP, respectively [8]. Glucose deprivation can increase the mutation rate of *KRAS* in CRC, which facilitates glucose uptake through the induction of GLUT1 [9]. Moreover, in *KRAS*-mutant CRC cell lines, vitamin C treatment was recently shown to induce a substantial increase in endogenous reactive oxygen species mediated by increased uptake of the oxidized vitamin C through GLUT1, which inhibited glycolysis at GAPDH to result in an energy crisis and ultimately cell death [33]. We previously reported that glucose uptake, as measured by FDG positron emission tomography scans, was associated with *KRAS* mutations and GLUT1 expression in primary and metastatic CRCs [10,12] and that *KRAS*-mutant CRC cells increased FDG accumulation by upregulating GLUT1 and HIF-1α under hypoxic conditions [11]. Tumorigenesis induced by mutated *KRAS* was also shown to be dependent on the function of mitochondria to generate reactive oxygen species, particularly through elevated glutamine metabolism [34]. In the present study, using comprehensive CE/MS metabolomics analysis, we found that mutated *KRAS* significantly altered the amino acid metabolism of CRC cells (Figure 1*A* and Supplementary Figure S1*A*). Most importantly, mutated *KRAS* markedly decreased the aspartate level and increased the asparagine level (Figure 1*B* and Supplementary Figure S1*B*). In addition, we demonstrated that the expression of ASNS, the enzyme that synthesizes asparagine from aspartate, was upregulated by mutated *KRAS* in CRC using multiple human CRC cell lines and clinical specimens of human primary CRC (Figure 2, *B*–*D*) and that ASNS expression was regulated by a *KRAS*-activated pathway, specifically the PI3K-AKT-mTOR pathway (Figure 2*A*). ASNS was reported to be activated by mutated p53, protein limitation, and tumor microenvironment stress [35–37]. ASNS was reported to be associated with the sensitivity of L-Asp in the treatment of ALL [35,38]. In addition, ASNS was also reported to be associated with the sensitivity of cisplatin and with clinical prognosis in some types of solid cancer [20,24,39–42]. To our knowledge, this is the first study to investigate the relationship between CRC and ASNS.

In addition to the well-established role of an altered glucose metabolism in cancer, recent studies have also elucidated the role of amino acid metabolism, especially glutamine, in cell proliferation and maintenance [13,14]. Although the molecular mechanism of glutamine addiction in cancer cells is unknown, several oncogenic mutations or

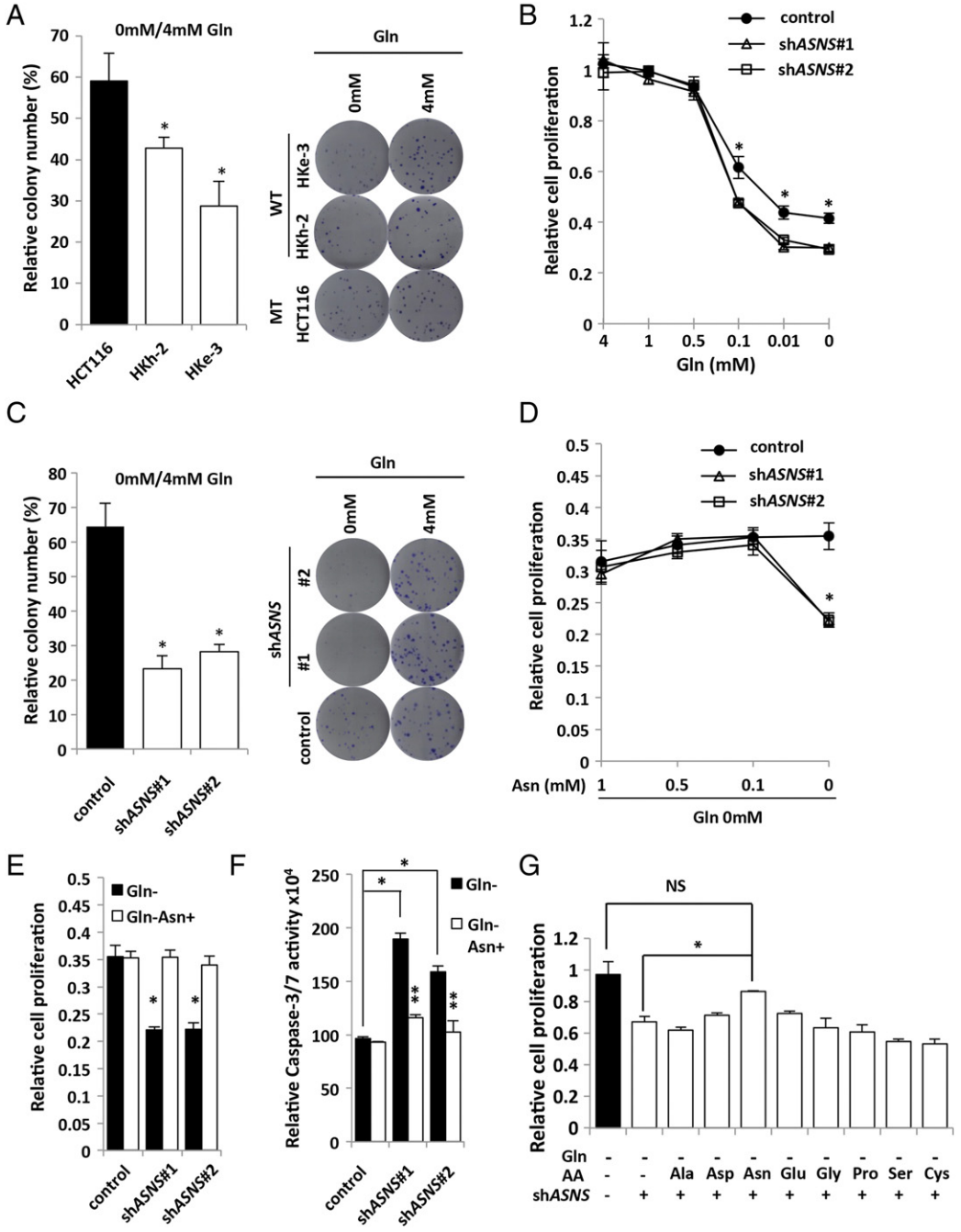

Figure 3. ASNS maintains cell adaptation to glutamine depletion in *KRAS*-mutant CRC cells. (A) Clonogenic assay with HCT116 and their isogenic wild-type *KRAS* cells (HKh-2 and HKe-3). Cells were maintained under 4 mM or 0 mM glutamine (Gln) condition containing 10% FBS for 10 days. Each colony number in 0 mM Gln was normalized to that in 4 mM Gln. Mean; *bars,* ± SD, $n = 3$ (Student's *t* test; $*P < .05$). (B) Cell proliferation measured by CCK-8 assay. HCT116 cells transfected with control or two independent sh*ASNS* vectors were maintained under various Gln concentration containing 10% FBS for 48 hours. Viability in each condition was normalized to that in 4 mM Gln. Student's *t* test; $*P < .05$. (C) Clonogenic assay with HCT116 transfected with control or two independent sh*ASNS* vectors. Cells were maintained under 4 or 0 mM Gln condition containing 10% FBS for 10 days. Each colony number in 0 mM Gln was normalized to that in 4 mM Gln. Mean; *bars,* ± SD, $n = 3$ (Student's *t* test; $*P < .05$). (D) Cell proliferation measured by CCK-8 assay. HCT116 transfected with control or two independent sh*ASNS* vectors. Cells were maintained under various concentrations of Asn and 0 mM Gln containing 10% FBS for 48 hours. Viability in each condition was normalized to that in 4 mM Gln. Student's *t* test; $*P < .05$. (E) Cell proliferation measured by CCK-8 assay. HCT116 cells transfected with control or two independent shASNS vectors were maintained under either 0 mM Gln or 0 mM Gln + 0.1 mM Asn containing 10% FBS for 48 hours. Viability in each condition was normalized to that in 4 mM Gln. Mean; *bars,* ± SD, $n = 3$ (Student's *t* test; $*P < .05$). (F) Caspase 3/7 activities. HCT116 transfected with control or two independent sh*ASNS* vectors were maintained under either 0 mM Gln or 0 mM Gln + 1 mM Asn containing 10% FBS for 48 hours. Caspase 3/7 activity was normalized to the cell viability measured by CCK-8 assay under the same density and conditions. Mean; *bars,* ± SD, $n = 3$ (Student's *t* test; $*P < .05$, control vector versus sh*ASNS* vectors; $**P < .05$, 0 mM Gln versus 0 mM Gln+ 1 mM Asn). (G) Cell proliferation measured by CCK-8 assay. HCT116 cells transfected with control or sh*ASNS* vectors were maintained under 0 mM Gln plus each amino acid (0.5 mM) containing 10% FBS for 48 hours. Viability in each condition was normalized to that in 4 mM Gln. Mean; *bars,* ± SD, $n = 3$ (Student's *t* test; $*P < .05$, NS: not significant).

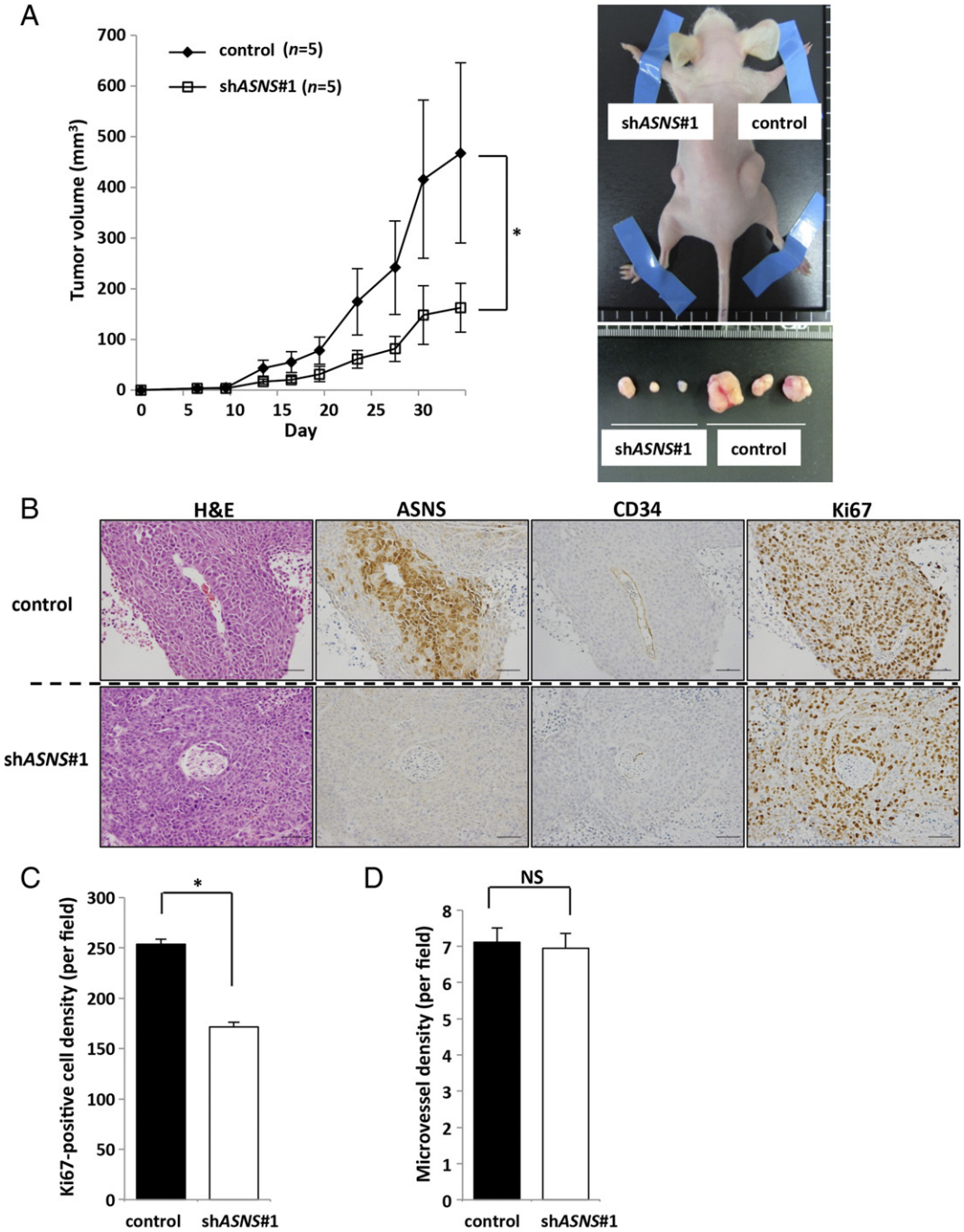

Figure 4. ASNS knockdown inhibits tumor growth *in vivo.* (A) Xenograft size of HCT116 cells transfected with control or sh*ASNS* vector. A total of 4×10^6 cells were subcutaneously injected into the flank of 4- to 6-week-old female nude mice, and then tumor volumes were measured 2 times per week (each group, $n = 5$). Representative images of tumors are shown. (B) H&E and immumohistochemical staining for ASNS, CD34, and Ki67 in xenograft tumors. Upper panels show serial sections of control tumors, whereas lower panels show those of sh*ASNS*-transfected tumors. Scale bar, 50 μm. (C) Ki67-positive cell density. Cell numbers were counted in five random fields (each group, $n = 3$). Mean; *bars,* ± SD (Student's *t* test; $^*P < .05$). (D) Microvessel density. CD34-positive cells were counted in five random fields (each group, $n = 3$). Mean; *bars,* ± SD (Student's *t* test; NS: not significant).

alterations have been linked to glutamine dependency in cancers. For example, Myc is able to increase glutamine metabolism by upregulating GLS expression, which leads to glutamine entry into the TCA cycle as α-ketoglutarate [43]. Moreover, recent studies have revealed that PDCA, glioma, and neuroblastoma metabolize glutamine in a manner that is different from canonical GLUD1 pathway (conversion of glutamine-derived glutamate into α-ketoglutarate by GLUD1 to fuel the TCA cycle) [19,20]. In PDCA, mutated *KRAS* contributes to glutamine dependency by using glutamine-derived aspartate to produce oxaloacetate *via* GOT1 in the cytoplasm. Oxaloacetate is subsequently converted into malate and then to pyruvate to maintain a high $NADPH/NADP^+$ ratio for redox homeostasis [19]. In glioma and

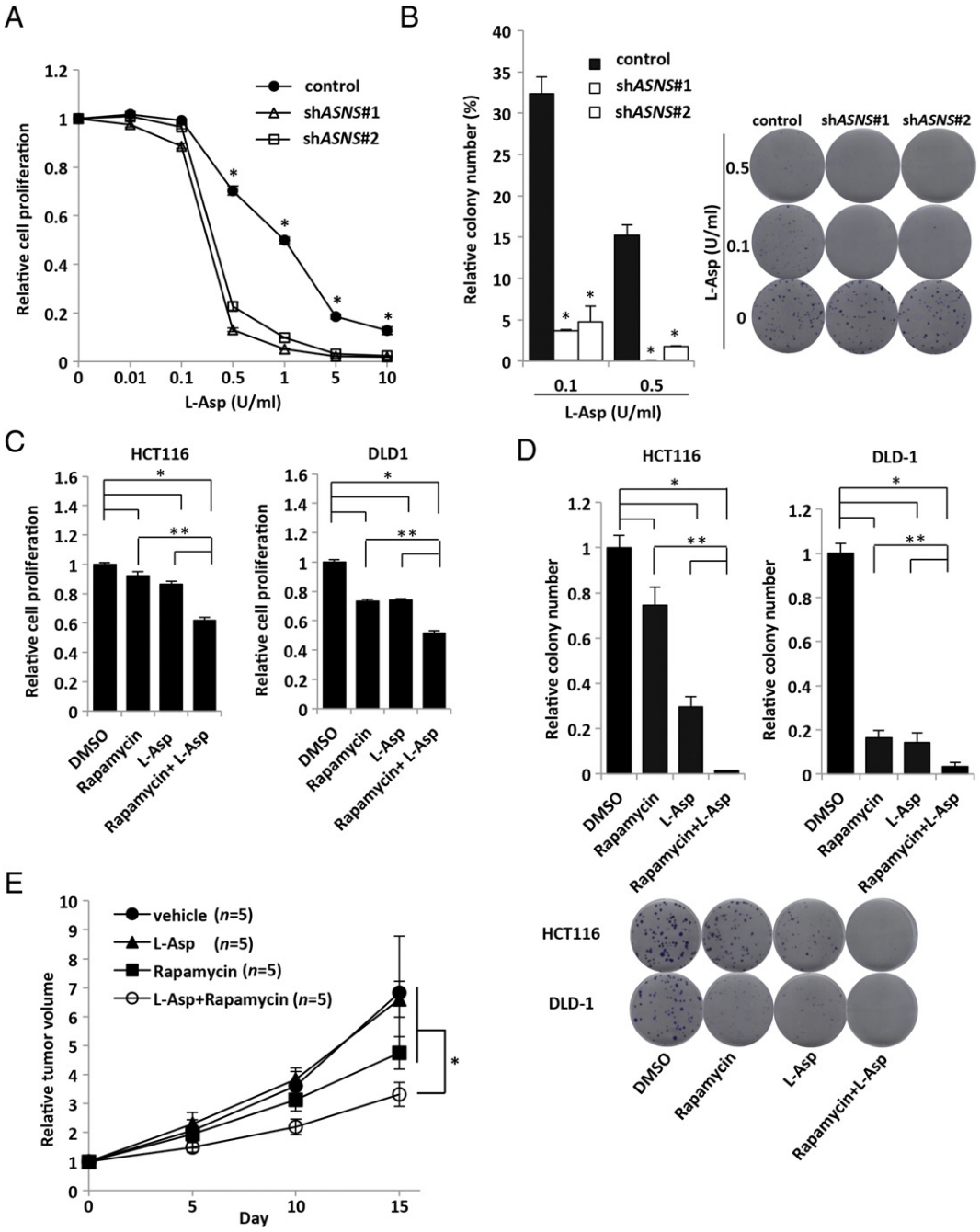

Figure 5. Inhibition of ASNS suppresses *in vivo* tumor growth of *KRAS*-mutant CRC cells. (A) Cell proliferation measured by CCK-8 assay. HCT116 cells transfected with control or two independent sh*ASNS* vectors were treated with various concentrations of L-Asp for 72 hours. Viability in each condition was normalized to the control. Mean; *bars,* ± SD, $n = 3$ (Student's *t* test; $*P < .05$). (B) Clonogenic assay with HCT116 transfected with control or two independent sh*ASNS* vectors. Cells were treated by various concentrations of L-Asp for 10 days. Each colony number was normalized to that under no treatment of L-Asp. Mean; *bars,* ± SD, $n = 3$ (Student's *t* test; $*P < .05$). (C) Cell proliferation measured by CCK-8 assay. HCT116 and DLD-1 cells were treated by DMSO, rapamycin (20 nM), L-Asp (0.25 U/ml), or rapamycin (20 nM) + L-Asp (0.25 U/ml) for 48 hours. Viability in each condition was normalized to that of DMSO treatment group. Mean; *bars*, ± SD, $n = 3$ (Student's *t* test; $*P < .05$, compared with DMSO treatment group; $**P < .05$, compared with combination treatment group [rapamycin + L-Asp]). (D) Clonogenic assay. HCT116 and DLD-1 cells were treated by DMSO, rapamycin (20 nM), L-Asp (0.1 U/ml), or rapamycin (20 nM) + L-Asp (0.1 U/ml). Each colony number was normalized to that of DMSO treatment group. Mean; *bars,* ± SD, $n = 3$ (Student's *t* test; $*P < .05$, compared with DMSO treatment group; $**P < .05$, compared with combination treatment group [rapamycin + L-Asp)]. (E) Xenograft size of HCT116 cells treated with vehicle, L-Asp, rapamycin, or L-Asp + rapamycin. HCT116 subcutaneously injected into the flank of 4- to 6-week-old female nude mice. Tumors of 150 to 300 mm^3 were randomly divides into 4 groups: vehicle, L-Asp alone (1500 U/kg), rapamycin alone (3 mg/kg), and combination of both drugs groups. We injected L-Asp daily and rapamycin every 5 days intraperitoneally for 15 days. Relative tumor volume was calculated based on the tumor volume at the start day of each treatment. Each group, $n = 5$. Mean; *bars,* ± SD, Student's *t* test; $*P < .05$, compared with combination treatment group (rapamycin + L-Asp).

neuroblastoma, CS RNAi knockdown prevents apoptosis induced by glutamine withdrawal by reducing TCA cycle activity and diverting oxaloacetate into aspartate and asparagine, which indicates that maintaining TCA cycle is not the primary mechanism of apoptosis suppression by glutamine metabolism. Glutamine-dependent asparagine synthesis by ASNS is required to suppress apoptosis induced by glutamine withdrawal [20]. However, the role of the glutamine metabolism in CRCs has not been fully elucidated. In the present study, we demonstrated that *KRAS*-mutant CRC cells could become adaptive to glutamine depletion through asparagine biosynthesis by ASNS and that addition of exogenous asparagine rescued the growth inhibition and cell death under the glutamine-free condition (Figure 3). It was recently reported that asparagine addition to glutamine-deprived cells altered the transcriptional response, thereby suppressing the induction of apoptotic regulators of the unfolded protein response effectors CHOP and XBP1 [20]. Moreover, a recent report has indicated that intracellular asparagine promotes cancer cell proliferation through uptake of amino acids (especially serine, arginine, and histidine) which are involved in protein and nucleotide synthesis [44]. Taken together, these results suggest important roles of asparagine in controlling protein synthesis and turnover in CRC. We observed that mutated *KRAS* did not alter the expression of GLUD1 and GOT1 in CRC (Figure 1, *D* and *F*), although mutated *KRAS* was reported to cause a decrease of GLUD1 and an increase of GOT1 in PDCA [19], indicating that the multifaceted roles of *KRAS* in metabolism are cell type dependent.

The importance of asparagine to cell survival has already been established through the use of L-Asp as a therapy for ALL. Leukemic cells lack the constitutive expression of ASNS and the ability to synthesize asparagine from glutamine and thus are dependent on exogenous asparagine to maintain their viability. In contrast, most solid tumors express ASNS and synthesize asparagine from glutamine [37], and L-Asp has not been proven as an effective therapy. The effects of ASNS in tumorigenesis also seem to be cell type dependent. It was recently reported that ASNS silencing produced the strongest inhibitory effect on sarcoma growth in a functional genomic shRNA-based screening of mouse sarcomas generated by oncogenic *KRAS* and disruption of *Cdkn2a*[22]. ASNS silencing in sarcoma cell lines reduced the percentage of S phase cells and impeded new polypeptide synthesis. The effects of ASNS silencing in sarcoma cells were reversed by exogenous supplementation of asparagine. Moreover, ASNS inhibition significantly slowed mouse sarcoma growth *in vivo* only when combined with asparaginase, implicating asparagine-promoted cellular adaptation to metabolic stress such as glutamine depletion. In the present study, ASNS inhibition significantly suppressed tumor growth *in vivo* of KRAS-mutant CRC cells (HCT116) (Figure 4*A* and Supplementary Figure S4*G*). Normal serum asparagine levels of mice and humans were reported to be 0.052 mM and 0.046 mM, respectively [22,45]. In sh*ASNS* transfectants, we found that the growth-inhibitory effects *in vitro* were recovered by exogenous addition of 0.1 mM asparagine (Figure 3, *D*–*G* and Supplementary Figure S5*A*). Therefore, we examined whether the physiological concentration of asparagine (i.e., 0.05 mM) could recover the growth-inhibitory effects and found that 0.05 mM asparagine was not sufficient to recover the growth inhibition *in vitro* (Supplementary Figure S5*C*). In addition, the tumor cells within solid tumors *in vivo* are under a state of poorer nutrient, especially in the regions distant from tumor blood vessels. L-Asp treatment could diminish serum asparagine levels of mice and humans down to 0.004 and 0 mM, respectively [22,45]. ASNS induction by L-Asp treatment was reported to be the resistance mechanism of L-Asp in the treatment of ALL [46]. Currently, ASNS inhibition has only been tested in L-Asp–refractory cases of ALL. ASNS inhibition induced cell death of glioblastoma cell lines in culture only when exogenous asparagine was absent [20]. Such inhibitors may well exhibit a therapeutic effect in other cancers when used together with L-Asp. A potent ASNS inhibitor available for use *in vivo* has not been developed yet [20,29,30] and is desirable clinically. In the present study, we found that L-Asp alone was not effective to *KRAS*-mutant xenografts (Figure 5*E*) and that ASNS protein expression was upregulated upon treatment with in the L-Asp alone (Supplementary Figure S6, *A* and *B*). We also demonstrated that rapamycin significantly suppressed ASNS expression *in vitro* and *in vivo* (Figure 2*A* and Supplementary Figure S6, *A* and *B*) and that the combination of L-Asp plus rapamycin markedly suppressed tumor growth *in vivo* (Figure 5*E*). Taken together, these results suggest that the combination of L-Asp plus rapamycin might be effective even in CRC with elevated ASNS expression. L-Asp and a rapamycin derivative, temsirolimus, were approved by FDA for the treatment of ALL and renal cell carcinoma, respectively [27,28,47]. It is notable that the safety of L-Asp and temsirolimus has already been assessed in these targeted diseases. However, native L-Asp derived from *Escherichia coli* cannot be acceptable in adult solid cancer patients due to its side effect [41]. A new L-Asp encapsulated within erythrocytes appears to improve safety compared with the native L-Asp [48], and a clinical trial is ongoing to evaluate the new L-Asp in PDCA metastatic setting [32]. Furthermore, chemical targeting of asparagine availability can also have a therapeutic value in several types of solid tumors including CRC.

Supplementary data to this article can be found online at http://dx.doi.org/10.1016/j.neo.2016.09.004.

Authors' Contributors

Conception and design: K. Kawada.

Development of methodology: K. Toda, M. Iwamoto.

Acquisition of data: K. Toda, M. Iwamoto, S. Inamoto.

Analysis and interpretation of data: K. Kawada, K. Toda, S. Inamoto.

Writing, review, and/or revision of the manuscript: K. Kawada, K. Toda, M. Iwamoto, S. Inamoto, T. Sasazuki, S. Shirasawa, S. Hasegawa.

Administrative, technical, or material support: T. Sasazuki, S. Shirasawa, S. Hasegawa.

Study supervision: K. Kawada, Y. Sakai.

References

[1] Jonker DJ, O'Callaghan CJ, Karapetis CS, Zalcberg JR, Tu D, Au HJ, Berry SR, Krahn M, Price T, and Simes RJ, et al (2007). Cetuximab for the treatment of colorectal cancer. *N Engl J Med* **357**, 2040–2048.

[2] Karapetis CS, Khambata-Ford S, Jonker DJ, O'Callaghan CJ, Tu D, Tebbutt NC, Simes RJ, Chalchal H, Shapiro JD, and Robitaille S, et al (2008). K-ras mutations and benefit from cetuximab in advanced colorectal cancer. *N Engl J Med* **359**, 1757–1765.

[3] Ye LC, Liu TS, Ren L, Wei Y, Zhu DX, Zai SY, Ye QH, Yu Y, Xu B, and Qin XY, et al (2013). Randomized controlled trial of cetuximab plus chemotherapy for patients with KRAS wild-type unresectable colorectal liver-limited metastases. *J Clin Oncol* **31**, 1931–1938.

[4] Vander Heiden MG, Cantley LC, and Thompson CB (2009). Understanding the Warburg effect: the metabolic requirements of cell proliferation. *Science* **324**, 1029–1033.

[5] Koppenol WH, Bounds PL, and Dang CV (2011). Otto Warburg's contributions to current concepts of cancer metabolism. *Nat Rev Cancer* **11**, 325–337.

[6] Cairns RA, Harris IS, and Mak TW (2011). Regulation of cancer cell metabolism. *Nat Rev Cancer* **11**, 85–95.

[7] Galluzzi L, Kepp O, Vander Heiden MG, and Kroemer G (2013). Metabolic targets for cancer therapy. *Nat Rev Drug Discov* **12**, 829–846.

[8] Ying H, Kimmelman AC, Lyssiotis CA, Hua S, Chu GC, Fletcher-Sananikone E, Locasale JW, Son J, Zhang H, and Coloff JL, et al (2012). Oncogenic Kras maintains pancreatic tumors through regulation of anabolic glucose metabolism. *Cell* **149**, 656–670.

[9] Yun J, Rago C, Cheong I, Pagliarini R, Angenendt P, Rajagopalan H, Schmidt K, Willson JK, Markowitz S, and Zhou S, et al (2009). Glucose deprivation contributes to the development of KRAS pathway mutations in tumor cells. *Science* **325**, 1555–1559.

[10] Kawada K, Nakamoto Y, Kawada M, Hida K, Matsumoto T, Murakami T, Hasegawa S, Togashi K, and Sakai Y (2012). Relationship between 18F-fluorodeoxyglucose accumulation and KRAS/BRAF mutations in colorectal cancer. *Clin Cancer Res* **18**, 1696–1703.

[11] Iwamoto M, Kawada K, Nakamoto Y, Itatani Y, Inamoto S, Toda K, Kimura H, Sasazuki T, Shirasawa S, and Okuyama H, et al (2014). Regulation of 18F-FDG accumulation in colorectal cancer cells with mutated KRAS. *J Nucl Med* **55**, 2038–2044.

[12] Kawada K, Toda K, Nakamoto Y, Iwamoto M, Hatano E, Chen F, Hasegawa S, Togashi K, Date H, and Uemoto S, et al (2015). Relationship between 18F-FDG PET/CT scans and KRAS mutations in metastatic colorectal cancer. *J Nucl Med* **56**, 1322–1327.

[13] Wise DR and Thompson CB (2010). Glutamine addiction: a new therapeutic target in cancer. *Trends Biochem Sci* **35**, 427–433.

[14] DeBerardinis RJ and Cheng T (2010). Q's next: the diverse functions of glutamine in metabolism, cell biology and cancer. *Oncogene* **29**, 313–324.

[15] Kovacevic Z and Morris HP (1972). The role of glutamine in the oxidative metabolism of malignant cells. *Cancer Res* **32**, 326–333.

[16] Le A, Lane AN, Hamaker M, Bose S, Gouw A, Barbi J, Tsukamoto T, Rojas CJ, Slusher BS, and Zhang H, et al (2012). Glucose-independent glutamine metabolism via TCA cycling for proliferation and survival in B cells. *Cell Metab* **15**, 110–121.

[17] Timmerman LA, Holton T, Yuneva M, Louie RJ, Padro M, Daemen A, Hu M, Chan DA, Ethier SP, and van 't Veer LJ, et al (2013). Glutamine sensitivity analysis identifies the xCT antiporter as a common triple-negative breast tumor therapeutic target. *Cancer Cell* **24**, 450–465.

[18] Wang JB, Erickson JW, Fuji R, Ramachandran S, Gao P, Dinavahi R, Wilson KF, Ambrosio AL, Dias SM, and Dang CV, et al (2010). Targeting mitochondrial glutaminase activity inhibits oncogenic transformation. *Cancer Cell* **18**, 207–219.

[19] Son J, Lyssiotis CA, Ying H, Wang X, Hua S, Ligorio M, Perera RM, Ferrone CR, Mullarky E, and Shyh-Chang N, et al (2013). Glutamine supports pancreatic cancer growth through a KRAS-regulated metabolic pathway. *Nature* **496**, 101–105.

[20] Zhang J, Fan J, Venneti S, Cross JR, Takagi T, Bhinder B, Djaballah H, Kanai M, Cheng EH, and Judkins AR, et al (2014). Asparagine plays a critical role in regulating cellular adaptation to glutamine depletion. *Mol Cell* **56**, 205–218.

[21] Shirasawa S, Furuse M, Yokoyama N, and Sasazuki T (1993). Altered growth of human colon cancer cell lines disrupted at activated Ki-ras. *Science* **260**, 85–88.

[22] Hettmer S, Schinzel AC, Tchessalova D, Schneider M, Parker CL, Bronson R, Richards NG, Hahn W, and Wagers AJ (2015). Functional genomic screening reveals asparagine dependence as a metabolic vulnerability in sarcoma. *Elife* **4**.

[23] Pencreach E, Guerin E, Nicolet C, Lelong-Rebel I, Voegeli AC, Oudet P, Larsen AK, Gaub MP, and Guenot D (2009). Marked activity of irinotecan and rapamycin combination toward colon cancer cells in vivo and in vitro is mediated through cooperative modulation of the mammalian target of rapamycin/hypoxia-inducible factor-1alpha axis. *Clin Cancer Res* **15**, 1297–1307.

[24] Zhang B, Dong LW, Tan YX, Zhang J, Pan YF, Yang C, Li MH, Ding ZW, Liu LJ, and Jiang TY, et al (2013). Asparagine synthetase is an independent predictor of surgical survival and a potential therapeutic target in hepatocellular carcinoma. *Br J Cancer* **109**, 14–23.

[25] Markowitz S, Wang J, Myeroff L, Parsons R, Sun L, Lutterbaugh J, Fan RS, Zborowska E, Kinzler KW, and Vogelstein B, et al (1995). Inactivation of the type II TGF-beta receptor in colon cancer cells with microsatellite instability. *Science* **268**, 1336–1338.

[26] Morin PJ, Sparks AB, Korinek V, Barker N, Clevers H, Vogelstein B, and Kinzler KW (1997). Activation of beta-catenin-Tcf signaling in colon cancer by mutations in beta-catenin or APC. *Science* **275**, 1787–1790.

[27] Chan WK, Lorenzi PL, Anishkin A, Purwaha P, Rogers DM, Sukharev S, Rempe SB, and Weinstein JN (2014). The glutaminase activity of L-asparaginase is not required for anticancer activity against ASNS-negative cells. *Blood* **123**, 3596–3606.

[28] Narta UK, Kanwar SS, and Azmi W (2007). Pharmacological and clinical evaluation of L-asparaginase in the treatment of leukemia. *Crit Rev Oncol Hematol* **61**, 208–221.

[29] Gutierrez JA, Pan YX, Koroniak L, Hiratake J, Kilberg MS, and Richards NG (2006). An inhibitor of human asparagine synthetase suppresses proliferation of an L-asparaginase-resistant leukemia cell line. *Chem Biol* **13**, 1339–1347.

[30] Ikeuchi H, Ahn YM, Otokawa T, Watanabe B, Hegazy L, Hiratake J, and Richards NG (2012). A sulfoximine-based inhibitor of human asparagine synthetase kills L-asparaginase–resistant leukemia cells. *Bioorg Med Chem* **20**, 5915–5927.

[31] Bryant KL, Mancias JD, Kimmelman AC, and Der CJ (2014). KRAS: feeding pancreatic cancer proliferation. *Trends Biochem Sci* **39**, 91–100.

[32] Cohen R, Neuzillet C, Tijeras-Raballand A, Faivre S, de Gramont A, and Raymond E (2015). Targeting cancer cell metabolism in pancreatic adenocarcinoma. *Oncotarget* **6**, 16832–16847.

[33] Yun J, Mullarky E, Lu C, Bosch KN, Kavalier A, Rivera K, Roper J, Chio II, Giannopoulou EG, and Rago C, et al (2015). Vitamin C selectively kills KRAS and BRAF mutant colorectal cancer cells by targeting GAPDH. *Science* **325**, 1555–1559.

[34] Weinberg F, Hamanaka R, Wheaton WW, Weinberg S, Joseph J, Lopez M, Kalyanaraman B, Mutlu GM, Budinger GR, and Chandel NS (2010). Mitochondrial metabolism and ROS generation are essential for Kras-mediated tumorigenicity. *Proc Natl Acad Sci U S A* **107**, 8788–8793.

[35] Scian MJ, Stagliano KE, Deb D, Ellis MA, Carchman EH, Das A, Valerie K, Deb SP, and Deb S (2004). Tumor-derived p53 mutants induce oncogenesis by transactivating growth-promoting genes. *Oncogene* **23**, 4430–4443.

[36] Ye J, Kumanova M, Hart LS, Sloane K, Zhang H, De Panis DN, Bobrovnikova-Marjon E, Diehl JA, Ron D, and Koumenis C (2010). The GCN2-ATF4 pathway is critical for tumour cell survival and proliferation in response to nutrient deprivation. *EMBO J* **29**, 2082–2096.

[37] Balasubramanian MN, Butterworth EA, and Kilberg MS (2013). Asparagine synthetase: regulation by cell stress and involvement in tumor biology. *Am J Physiol Endocrinol Metab* **304**, E789-799.

[38] Richards NG and Kilberg MS (2006). Asparagine synthetase chemotherapy. *Annu Rev Biochem* **75**, 629–654.

[39] Cui H, Darmanin S, Natsuisaka M, Kondo T, Asaka M, Shindoh M, Higashino F, Hamuro J, Okada F, and Kobayashi M, et al (2007). Enhanced expression of asparagine synthetase under glucose-deprived conditions protects pancreatic cancer cells from apoptosis induced by glucose deprivation and cisplatin. *Cancer Res* **67**, 3345–3355.

[40] Lorenzi PL, Llamas J, Gunsior M, Ozbun L, Reinhold WC, Varma S, Ji H, Kim H, Hutchinson AA, and Kohn EC, et al (2008). Asparagine synthetase is a predictive biomarker of L-asparaginase activity in ovarian cancer cell lines. *Mol Cancer Ther* **7**, 3123–3128.

[41] Dufour E, Gay F, Aguera K, Scoazec JY, Horand F, Lorenzi PL, and Godfrin Y (2012). Pancreatic tumor sensitivity to plasma L-asparagine starvation. *Pancreas* **41**, 940–948.

[42] Sircar K, Huang H, Hu L, Cogdell D, Dhillon J, Tzelepi V, Efstathiou E, Koumakpayi IH, Saad F, and Luo D, et al (2012). Integrative molecular profiling reveals asparagine synthetase is a target in castration-resistant prostate cancer. *Am J Pathol* **180**, 895–903.

[43] Gao P, Tchernyshyov I, Chang TC, Lee YS, Kita K, Ochi T, Zeller KI, De Marzo AM, Van Eyk JE, and Mendell JT, et al (2009). c-Myc suppression of miR-23a/b enhances mitochondrial glutaminase expression and glutamine metabolism. *Nature* **458**, 762–765.

[44] Krall AS, Xu S, Graeber TG, Braas D, and Christofk HR (2016). Asparagine promotes cancer cell proliferation through use as an amino acid exchange factor. *Nat Commun* **7**, 11457.

[45] Minowa K, Suzuki M, Fujimura J, Saito M, Koh K, Kikuchi A, Hamada R, and Shimizu T (2012). L-asparaginase-induced pancreatic injury is associated with an imbalance in plasma amino acid levels. *Drugs R D* **12**, 49–55.

[46] Aslanian AM, Fletcher BS, and Kilberg MS (2001). Asparagine synthetase expression alone is sufficient to induce l-asparaginase resistance in MOLT-4 human leukaemia cells. *Biochem J* **357**, 321–328.

[47] Chiarini F, Evangelisti C, McCubrey JA, and Martelli AM (2015). Current treatment strategies for inhibiting mTOR in cancer. *Trends Pharmacol Sci* **36**, 124–135.

[48] Domenech C, Thomas X, Chabaud S, Baruchel A, Gueyffier F, Mazingue F, Auvrignon A, Corm S, Dombret H, and Chevallier P, et al (2011). L-asparaginase loaded red blood cells in refractory or relapsing acute lymphoblastic leukaemia in children and adults: results of the GRASPALL 2005-01 randomized trial. *Br J Haematol* **153**, 58–65.